

## THEORIES OF FERMION MASSES\*

JONATHAN BAGGER

*Stanford Linear Accelerator Center  
Stanford University, Stanford, California 94305*

SAVAS DIMOPOULOS†

*Department of Physics, Stanford University  
Stanford, California 94305*

HOWARD GEORGI

*Department of Physics, Harvard University  
Cambridge, Massachusetts 02138*

STUART RABY

*Theory Division, Los Alamos National Laboratory  
Los Alamos, New Mexico 87545*

### Abstract

We present grand unified theories in which the quark masses and mixing angles are calculated in terms of the lepton masses through simple group theory. The theories contain no small Yukawa couplings. A favored value of the top quark mass is 35 GeV.

---

\*Presented by S. Dimopoulos. Work supported by the Department of Energy, contract DE-AC03-76SF00515, and by the National Science Foundation, contracts NSF-PHY-83-10654 and NSF-PHY-82-15249.

†Alfred P. Sloan Foundation Fellow.

Invited Talk Presented at the Fifth Workshop on Grand Unification, Providence, Rhode Island, April 12-14, 1984

## Regularities

The fermion mass spectrum remains one of the outstanding problems of grand unification. Conventional grand unified theories<sup>1)</sup> offer no explanation for the immense range of quark and lepton masses. Nor do they shed any light on the magnitudes of the quark mixing angles. Conventional grand unified theories reproduce the observed fermion masses and mixings by introducing at least 13 parameters whose magnitudes range between 1 and  $10^{-6}$ .

The striking regularities of the fermion spectrum provide important insights into the question of fermion masses. The fermions cluster into groups of similar mass, called families, and this tendency to cluster is greatest at energies near the grand unified scale  $M_{GUT}$ . There are strong correlations between proximity in mass and the strength of the weak interactions. The weak partner of the lightest up-type quark is predominantly the lightest down-type quark, and similarly for the other families. In addition, nearest-neighbor families interact more strongly than families further removed.

Many of these regularities are incorporated into the Fritsch mass matrix,<sup>2)</sup>

$$M = m \begin{pmatrix} 1 & \theta & 0 \\ \theta & 0 & \theta^3 \\ 0 & \theta^3 & 0 \end{pmatrix}, \quad (1)$$

where  $\theta \lesssim 1$ . The Fritsch matrix has eigenvalues in the ratio  $1 : \theta^2 : \theta^4$ , and consecutive mixings of order  $\theta$ . In a theory based on a Fritsch-type matrix, the heaviest generation gets a direct mass, and subsequent families gain mass through mixings with their nearest neighbors.

Mass matrices with the Fritsch texture work well for the mass ratios

$$\theta^2 \sim \frac{d}{s} \sim \frac{s}{b} \sim \frac{\mu}{\tau} \sim \frac{1}{20}, \quad (2)$$

but are less successful for

$$\theta^2 \not\sim \frac{\mu}{c} \sim \frac{e}{\mu} \sim \frac{1}{200}. \quad (3)$$

Important challenges to the model builder include fixing the unsuccessful relations (3), and explaining the zero entries and the  $1 - \theta - \theta^3$  pattern of the Fritzsche mass matrix.

### A General Scenario

In this section we shall describe a general scenario for constructing theories with Fritzsche mass matrices.<sup>3]</sup> We shall focus on theories with three families, which we label by 1, 2 and 3 in Figure 1. To distinguish the families, we introduce a global U(1) family symmetry, with charges -4, 1 and 0 on the first, second and third families.

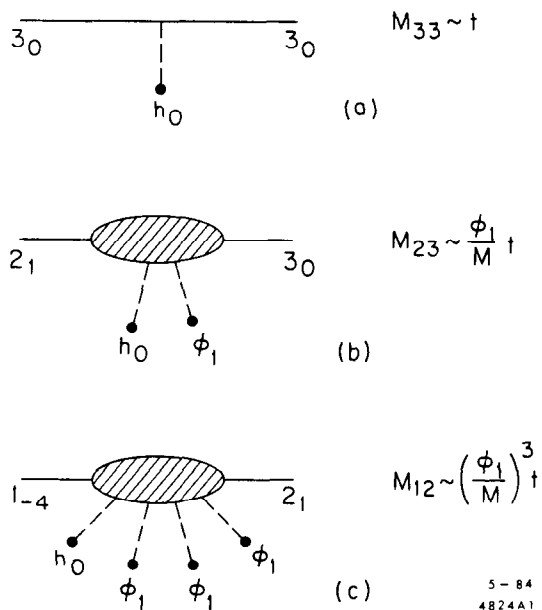


FIGURE 1: Diagrams that give rise to three-family Fritzsche matrices.

Since we would like the third family to get a direct mass, we give the weak Higgs doublet  $h_0$  family charge 0. This lets the vacuum expectation value  $\langle h_0 \rangle$  give an unsuppressed direct mass to the third family through the dimension-four operator of Figure 1a.

The second and third families mix through the diagram of Figure 1b. This mixing breaks the U(1) family symmetry by one unit, so Figure 1b involves an extra Higgs scalar  $\phi_1$ , where  $\phi_1$  carries one unit of family charge. This graph induces a dimension-five operator, suppressed by the ratio  $\langle \phi_1 \rangle$  over  $M$ , where  $M$  characterizes

the strength of the operator, and  $\langle\phi_1\rangle$  is the vacuum expectation value (vev) of the field  $\phi_1$ .

Similarly, the mixing of the first and second families breaks the U(1) family symmetry by three units, and is mediated by the dimension-seven operator shown in Figure 1c. (We assume that  $\phi_1$  is the only Higgs scalar that breaks the U(1) symmetry.) This implies that the mixing of the first and second families is suppressed by three powers of  $\langle\phi_1\rangle/M$ .

If we identify  $\langle\phi_1\rangle/M$  with the mixing angle  $\theta$ , the graphs of Figure 1 reproduce the nonzero entries of the Fritzsche mass matrix. If the graphs of Figure 1 are the *only* diagrams that contribute to the mass matrix, both the zeroes and the  $1 - \theta - \theta^3$  pattern of the Fritzsche matrix are explained naturally, without any small Yukawa couplings.

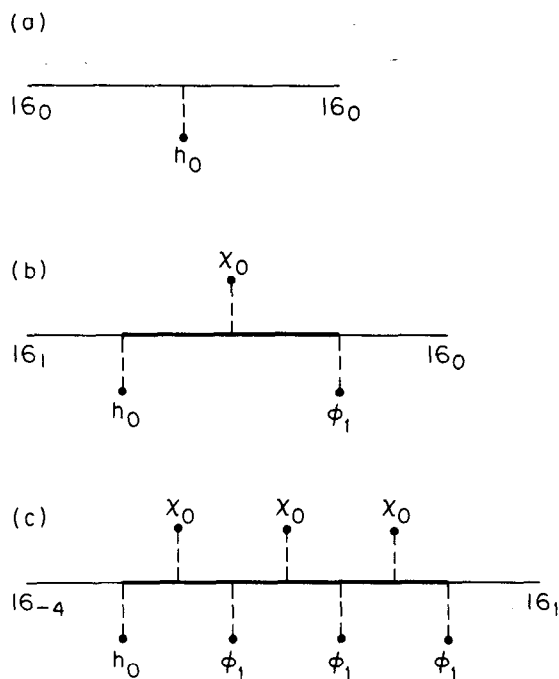
### An O(10) Example

To illustrate the previous scenario, we will construct an O(10) grand unified theory whose particle content and Yukawa couplings are summarized in Figure 2. We choose an O(10) theory because O(10) is the minimal grand unified group that relates the up, down and electron masses.

As before, the third family gets mass from the Weinberg-Salam Higgs doublet  $h_0$ . This is shown in Figure 2a, where the third family receives an unsuppressed direct mass  $m = g\langle h_0\rangle$ . The second and third families mix through a one-heavy-fermion intermediate state, as shown in Figure 2b. This graph is suppressed by  $\langle\phi_1\rangle/\langle\chi_0\rangle$ , where  $\langle\chi_0\rangle$  is the vev that gives mass to the heavy fermion. The first and second families mix through the graph of Figure 2c. This graph includes a three-heavy-fermion intermediate state, so it is suppressed by three powers of  $\langle\phi_1\rangle/\langle\chi_0\rangle$ . If we identify  $\langle\phi_1\rangle/\langle\chi_0\rangle$  with  $\theta$ , we obtain a mass matrix with Fritzsche texture. We will only consider theories where the vevs  $\langle\phi_1\rangle$  and  $\langle\chi_0\rangle$  are superlarge,\* so they must not break  $SU(3) \times SU(2) \times U(1)$ .

---

\* The vevs  $\langle\phi_1\rangle$  and  $\langle\chi_0\rangle$  must lie between  $10^8$  and  $10^{12}$  GeV because the family U(1) has color anomalies and gives rise to an "invisible" axion.



6-84

4824A2

FIGURE 2: Diagrams that give rise to three-family Fritzsch matrices for our  $O(10)$  theory. These graphs are in one-to-one correspondence with the diagrams of Figure 1. The heavy lines represent heavy fermions of mass between  $10^8$  and  $10^{12}$  GeV.

The graphs of Figure 2 define the complete quark and lepton mass matrices of our  $O(10)$  theory. One might hope that the quark and lepton masses could be computed in terms of three numbers, characterizing the overall scales of the three graphs. However, this is not usually the case, for the couplings of the fermions to the vevs depend, in general, on the unknown parameters of the Higgs potential. Our objective is to find conditions under which the couplings of the fermions to the vevs are given by simple group theory alone, and do not depend on the various parameters of the Higgs potential.

To see what is involved, let us consider the scalars  $\phi_1$  and  $\chi_0$ . Their vevs must lie in the  $SU(3) \times SU(2) \times U(1)$  preserving directions contained in  $16 \times \overline{16} = 1 + 45 + 210$ . There are six such directions, which we denote by  $1$ ,  $45_{B-L}$ ,  $45_Y$ ,

$210_{(B-L)^2}$ ,  $210_{Y(B-L)}$  and  $210_{Y^2}$ , where, for example,  $45_{B-L}$  points in the B - L direction of the adjoint of O(10). In general, we have

$$\langle \phi_1 \rangle = \alpha 1 + \beta 45_{B-L} + \gamma 45_Y + \delta 210_{(B-L)^2} + \epsilon 210_{Y(B-L)} + \zeta 210_{Y^2} \quad , \quad (4)$$

and similarly for  $\langle \chi_0 \rangle$ . The coefficients  $\alpha, \beta, \gamma, \delta, \epsilon$  and  $\zeta$  cannot be calculated from pure group theory; they depend on the details of the Higgs potential.

This situation can be improved if  $\phi_1$  and  $\chi_0$  belong to *irreducible* representations of O(10), either 1 or 45 or 210. However, this is not enough, for one still cannot distinguish between the different  $SU(3) \times SU(2) \times U(1)$  preserving directions contained in a single irreducible representation. For example, if  $\phi_1$  is a 45 under O(10), then

$$\langle \phi_1 \rangle = \alpha 45_{B-L} + \beta 45_Y \quad , \quad (5)$$

where  $\alpha$  and  $\beta$  still depend on the details of the Higgs potential. To remedy this problem we introduce the extended survival hypothesis,<sup>4]</sup> which ensures that either  $\alpha$  or  $\beta = 0$ .

### Extended Survival Hypothesis

We shall illustrate the extended survival hypothesis<sup>4]</sup> with a simple example, where we take  $\phi_1$  to be a 45 of O(10). We would like to ensure that  $\langle 45_Y \rangle \sim M_{GUT}$  and  $\langle 45_{B-L} \rangle \sim 0$ . How can we do this? If we break O(10) directly to  $SU(3) \times SU(2) \times U(1)$  at  $M_{GUT}$ , and give the  $45_Y$  a vev of order  $M_{GUT}$ , then mixings between the Y and B - L components of  $\phi_1$  will induce a similar vev for  $\langle 45_{B-L} \rangle$ . To avoid this problem, we shall consider the case where O(10) breaks to  $SU(3) \times SU(2) \times U(1)$  through an intermediate SU(5),

$$O(10) \xrightarrow{M_P} SU(5) \xrightarrow{M_{GUT}} SU(3) \times SU(2) \times U(1) \quad . \quad (6)$$

The  $45_{B-L}$  and the  $45_Y$  lie in *different* representations of  $SU(5)$ , so it is possible to make the  $45_{B-L}$  superheavy, with a mass of order  $M_P$ , and leave the  $45_Y$  light. At energies much less than  $M_P$ , the  $45_{B-L}$  is decoupled, so only the  $45_Y$  can get a significant vev,  $\langle 45_Y \rangle \sim M_{GUT}$ . Mixings will induce a vev for the  $45_{B-L}$ , but this will be suppressed by  $(M_{GUT}/M_P)^2$ .

The basic idea of the extended survival hypothesis is to introduce intermediate symmetries which interpolate between the initial and final symmetries. The intermediate symmetries allow one to split the desirable components of a representation from their undesirable counterparts. The extended survival hypothesis ensures that all vevs point in well-defined directions, and that these directions do not depend on the unknown parameters of the Higgs potential.

The extended survival hypothesis allows us to construct theories with calculable fermion masses. This is because each of the  $\phi_1$  and  $\chi_0$  vevs in Figure 2 can be arranged to point in precisely *one* of the six  $SU(3) \times SU(2) \times U(1)$  preserving directions, either 1,  $45_{B-L}$ ,  $45_Y$ ,  $210_{(B-L)^2}$ ,  $210_{Y(B-L)}$  or  $210_{Y^2}$ . This procedure leaves the overall scale of each graph undetermined. We choose to normalize the graphs in terms of the  $e$ ,  $\mu$  and  $\tau$  lepton masses. Once  $e$ ,  $\mu$  and  $\tau$  are specified, all the quark masses and mixing angles may be calculated by group theory alone.

The extended survival hypothesis may be readily applied to the three-family models of the previous section. The Fritsch matrices

$$M^a = m \begin{pmatrix} B^a & C_R^a \theta & 0 \\ C_L^a \theta & 0 & D_R^a \tilde{\theta}^3 \\ 0 & D_L^a \tilde{\theta}^3 & 0 \end{pmatrix} \quad (7)$$

give rise to masses and mixings of the following form,

$$\frac{t}{B^u} \simeq \frac{b}{B^d} \simeq \frac{\tau}{B^e}$$

$$\frac{ct}{C_L^u C_R^u} \simeq \frac{sb}{C_L^d C_R^d} \simeq \frac{\mu \tau}{C_L^e C_R^e}$$

$$\theta_{bs} \simeq \sqrt{\frac{C_L^d}{C_R^d}} \sqrt{\frac{s}{b}} \pm \sqrt{\frac{C_L^u}{C_R^u}} \sqrt{\frac{c}{t}}, \quad \text{etc.} \quad (8)$$

The coefficients  $m$ ,  $\theta$  and  $\tilde{\theta}$  are unknown. They are determined by fitting the  $e$ ,  $\mu$  and  $\tau$  masses. The prefactors  $B^a$ ,  $C_{L,R}^a$  and  $D_{L,R}^a$  are of order 1. They are calculated from group theory alone, and lead immediately to predictions for the quark masses and mixings in terms of  $e$ ,  $\mu$  and  $\tau$ .

### Dual Feynman Diagrams

Dual Feynman diagrams<sup>71</sup> are a convenient tool for constructing theories with Fritzsche mass matrices. Dual Feynman diagrams replace fermions (lines) by points, and vevs (points) by lines. In Figure 3 we summarize the graphical rules for dual Feynman diagrams.

|                          | Feynman<br>Notation | Dual<br>Notation |
|--------------------------|---------------------|------------------|
| Light Fermion            | —                   | ○                |
| Heavy Fermion            | —                   | ●                |
| $\langle h_0 \rangle$    | —● $h_0$            | ---              |
| $\langle \phi_1 \rangle$ | —● $\phi_1$         | —                |
| $\langle \chi_0 \rangle$ | —● $\chi_0$         | ==               |

6-84

4824A3

FIGURE 3: Rules for dual Feynman diagrams.

The dual Feynman diagrams of Figure 4 correspond to the ordinary Feynman diagrams of Figure 2. Note that each step of the dual Feynman diagram represents  $\langle \phi_1 \rangle / \langle \chi_0 \rangle$ , and costs one power of  $\theta$ .

The dual Feynman diagrams of Figure 4 may be joined together to form one large diagram, as shown in Figure 5. This diagram exhibits all the Yukawa couplings of the theory. The Fritzsche texture is manifest. Each step costs one power of  $\theta$ , and the Fritzsche zeroes follow from the topological properties of the graph.



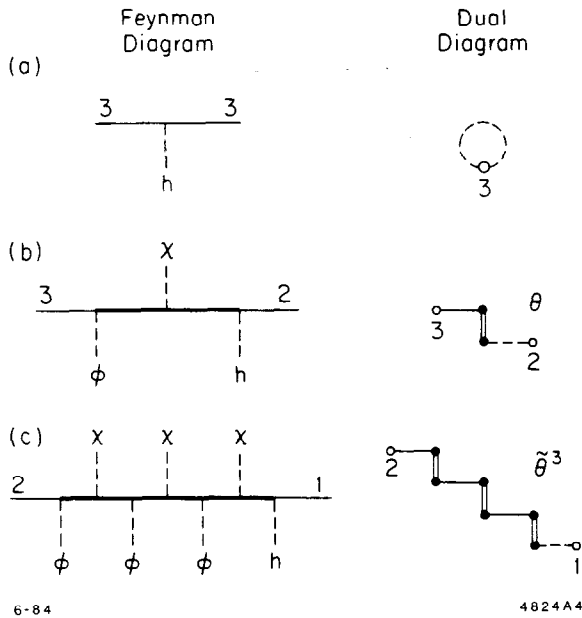


FIGURE 4: The correspondence between the Feynman and dual diagrams for the models of Figure 2. Note that each step in the dual diagram costs one power of  $\theta$  in the Fritzsche mass matrix.

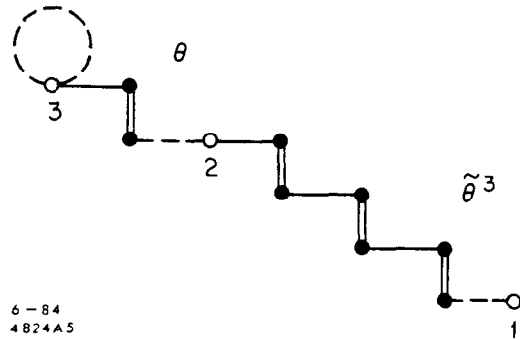


FIGURE 5: The dual Feynman diagram for our three-family  $O(10)$  theory.

### CAT Scanning

A given dual Feynman diagram represents not one theory, but many theories, depending on the directions in which the various vevs point. Each set of vevs gives a different set of predictions. Scanning over these vevs gives all possible predictions that arise from a given dual Feynman diagram. We refer to this procedure as Computer Assisted Theory Scanning, or CAT Scanning.<sup>7)</sup>

In this section we present results that arise from scanning the three-family  $O(10)$  models defined in Figures 6 and 7. These models were chosen because they naturally explain why  $\tau \ll M_W$ . We choose  $e$ ,  $\mu$  and  $\tau$  as inputs, and compute the quark masses and mixings in three stages:

- Round 1)  $t, b$
- Round 2)  $c, s, \theta_{bs}$
- Round 3)  $d/s, d/u, \theta_{sd}$ .

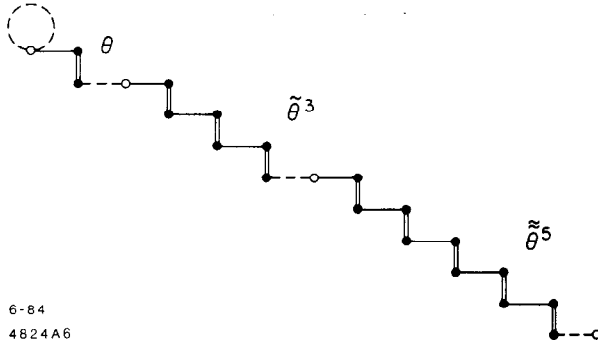


FIGURE 6: The dual diagram for the four-family model of Table 1. Note that the dashed links may be exchanged with the solid links immediately above. This gives rise to models with identical masses but different mixing angles.

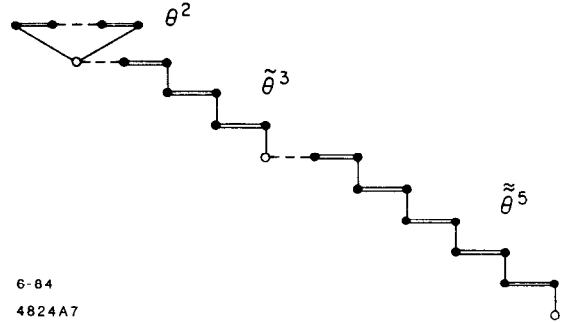


FIGURE 7: The dual diagram for the three-family model of Table 1. The triangle pattern explains why  $\tau \ll M_W$ .

After each round, we eliminate those models in conflict with experiment. The legoplots of Figure 8 illustrate this procedure for the first two rounds of the models defined in Figure 7. Tables 1 and 2 summarize the predictions of the best models that emerge from the scanning procedure.

As we see from Table 1, the agreement between theory and experiment is good<sup>5,6]</sup> for most values of  $b$ ,  $c$  and  $\theta_{bs}$ . The strange quark mass tends to be about twice the popular lower bound of  $.175 \pm .055$  GeV, which is extracted from QCD sum rules.<sup>5]</sup> The top quark mass takes values between 20 and 35 GeV.

The masses in Table 1 are renormalized from  $M_{GUT}$  assuming  $\Lambda_{\overline{MS}} = 100$  MeV. The values of the low energy masses are sensitive to this choice. For example, if  $\Lambda_{\overline{MS}}$  were 50 MeV, the four-family predictions for  $b$  and  $t$  would be reduced to 4.8 and 26 respectively.<sup>7]</sup>

In Table 2 we tabulate the predictions for  $s/d$ ,  $d/u$  and  $\theta_{sd}$  for the best models of Table 1. The predictions for  $\theta_{sd}$  and  $s/d$  are in good agreement with experiment. The results for  $d/u$  exclude the first two models. The predictions of our favorite models are underlined. The 22 GeV top quark mass is on the verge of being excluded by experiments at PETRA, so our favorite value for  $t$  is 35 GeV.

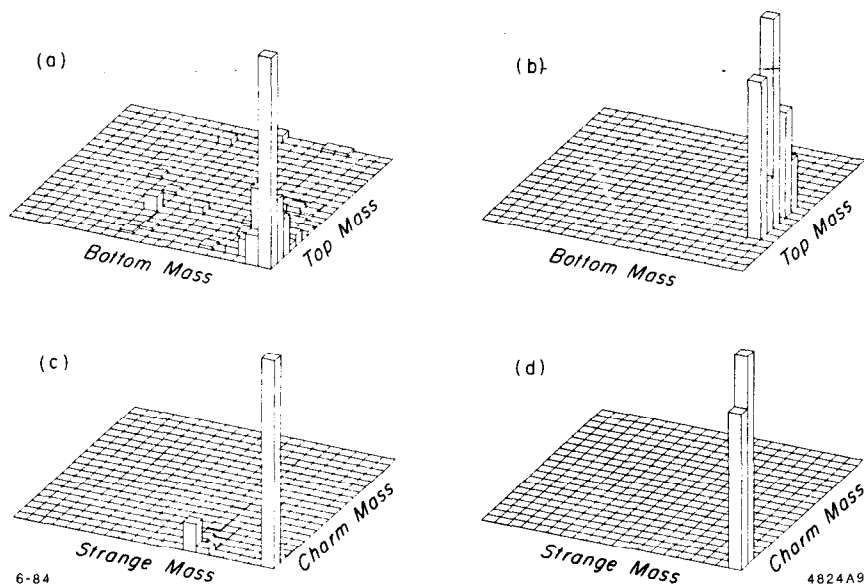


FIGURE 8: Legoplots summarizing the first and second rounds of CAT scanning for the models of Figure 7. The height of the plot is proportional to the number of theories with the indicated mass spectrum. *a)* Top and bottom masses, at the GUT scale, for the 1299 models considered in the first round of scanning. The masses are collected in 1 GeV bins. *b)* The same models after imposing cuts coming from experiment. Only 22 models survive the first round of cuts. *c)* Charm and strange masses, at the GUT scale, from the second round of scanning. The charm masses are collected in 250 MeV bins, and the strange masses in 100 MeV bins. The 230,320 models collected here follow from the 22 models that survived Round 1. *d)* The same models after imposing cuts. The cuts eliminate all but the 920 models shown here.

## Conclusions

We have found a framework which allows us to compute the quark masses and mixing angles in terms of the lepton masses, using simple group theory. We have scanned about  $10^6$  models, and several hundred give the predictions of Table 2. We are presently looking through these models to find those whose Higgs structure is appealing, and whose dual Feynman diagrams follow from simple family symmetries.

Our favored prediction for the top quark mass is 35 GeV.

TABLE 1. Results from the first two rounds of CAT Scanning for the models of Figures 6 and 7. The top, bottom and charm masses are evaluated at their respective masses, and  $s$  is evaluated at 1 GeV. For sake of comparison, the popular values for  $t$ ,  $b$ ,  $c$ ,  $s$  and  $\theta_{bs}$  are collected in the second row. Each of the subsequent rows contains the predictions of various classes of three- and four-family models.

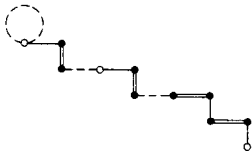
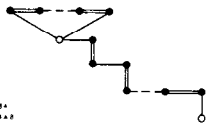
| Model   | $t(t)$         | $b(b)$       | $c(c)$       | $s(1\text{GeV})$ | $\theta_{bs}$  |
|---|----------------|--------------|--------------|------------------|----------------|
| popular values  | $t \gtrsim 22$ | $4.6 \pm .2$ | $1.2 \pm .1$ | $.175 \pm .055$  | $0.5 \pm .015$ |
| 4 – family<br>  | 29             | 5.3          | 1.7          | .39              | .07            |
|   | 29             | 5.3          | 1.2          | .39              | .03            |
|   | 29             | 5.3          | 1.2          | .39              | .06            |
|   | 29             | 5.3          | 1.2          | .39              | .05            |
| 3 – family<br> | 22             | 4.8          | 1.2          | .34              | .07            |
|   | 22             | 4.8          | 1.2          | .34              | .06            |
|   | 22             | 4.8          | 1.2          | .34              | .05            |
|   | 22             | 4.8          | 1.2          | .34              | .04            |
|   | 20             | 4.8          | 1.3          | .34              | .06            |
|   | 26             | 4.8          | 1.5          | .34              | .07            |
|   | 26             | 4.8          | 1.0          | .34              | .06            |
|   | 26             | 4.8          | 1.0          | .34              | .03            |
|   | 31             | 6.2          | 1.2          | .26              | .06            |
|   | 35             | 4.8          | 2.0          | .34              | .07            |
|   | 35             | 4.8          | 1.1          | .34              | .03            |

TABLE 2. Results from the third round of CAT scanning for selected models of Table 1. The predictions of the best models are underlined.

| $t(t)$         | $b(b)$       | $c(c)$       | $s(1\text{GeV})$ | $\theta_{be}$  | $s/d$      | $d/u$        | $\theta_{ed}$  |
|----------------|--------------|--------------|------------------|----------------|------------|--------------|----------------|
| $t \gtrsim 22$ | $4.6 \pm .2$ | $1.2 \pm .1$ | $.175 \pm .055$  | $.05 \pm .015$ | $20 \pm 2$ | $1.8 \pm .2$ | $.23 \pm .005$ |
| 29             | 5.3          | 1.7          | .39              | .05            | 23         | 1.0          | .23            |
| 26             | 4.8          | 1.5          | .34              | .07            | 23         | 1.0          | .23            |
| 35             | 4.8          | 2.0          | .34              | .07            | 16         | 1.4          | .19            |
| 35             | 4.8          | 1.1          | .34              | .03            | 16         | 1.4          | .25            |
| <u>35</u>      | <u>4.8</u>   | <u>1.1</u>   | <u>.34</u>       | <u>.03</u>     | <u>16</u>  | <u>1.4</u>   | <u>.23</u>     |
| 35             | 4.8          | 1.1          | .34              | .03            | 16         | 1.4          | .19            |
| 22             | 4.8          | 1.2          | .34              | .05            | 18         | 1.3          | .26            |
| <u>22</u>      | <u>4.8</u>   | <u>1.2</u>   | <u>.34</u>       | <u>.05</u>     | <u>18</u>  | <u>1.3</u>   | <u>.23</u>     |
| 22             | 4.8          | 1.2          | .34              | .05            | 18         | 1.3          | .18            |

### References

1. H. Georgi and S. Glashow, Phys. Rev. Lett. 32 (1974) 438; J. Pati and A. Salam, Phys. Rev. D10 (1974) 275.
2. H. Fritzsch, Nucl. Phys. B155 (1979) 189.
3. S. Dimopoulos, Phys. Lett. 129B (1983) 417.
4. S. Dimopoulos and H. Georgi, Stanford preprint ITP-759 (1984).
5. J. Gasser and H. Leutwyler, Phys. Rep. 87 (1982) 77.
6. L. Wolfenstein, Phys. Rev. Lett. 51 (1983) 1945.
7. J. Bagger, S. Dimopoulos and S. Raby, in preparation.